Embedding Human Knowledge into Deep Neural Network via Attention Map

Masahiro Mitsuhara, Hiroshi Fukui, Yusuke Sakashita, Takanori Ogata, Tsubasa Hirakawa, Takayoshi Yamashita and Hironobu Fujiyoshi
Chubu University, Kasugai, Aichi, Japan

Keywords: Visual Explanation, Human-in-the-Loop, Attention Mechanism, Object Recognition, Fine-grained Recognition.

Abstract: The conventional method to embed human knowledge has been applied for non-deep machine learning. Meanwhile, it is challenging to apply it for deep learning models due to the enormous number of model parameters. In this paper, we propose a novel framework for optimizing networks while embedding human knowledge. The crucial factors are an attention map for visual explanation and an attention mechanism. A manually edited attention map, in which human knowledge is embedded, has the potential to adjust recognition results. The proposed method updates network parameters so that the output attention map corresponds to the edited ones. As a result, the trained network can output an attention map that takes into account human knowledge. Experimental results with ImageNet, CUB-200-2010, and IDRiD demonstrate that it is possible to obtain a clear attention map for a visual explanation and improve the classification performance.

1 INTRODUCTION

Visual explanation is often used to interpret the decision-making of deep learning in the computer vision field (Ribeiro et al., 2016; Chattopadhay et al., 2018; Ramprasaath et al., 2017; Smilkov et al., 2017; Zeiler and Fergus, 2014; Zhou et al., 2016; Fukui et al., 2019; Montavon et al., 2018; Springenberg et al., 2015; Fong and Vedaldi, 2017; Petsiuk et al., 2018; Jetley et al., 2018). Visual explanation analyzes the decision-making of a convolutional neural network (CNN) (LeCun et al., 1989) by visualizing an attention map that highlights discriminative regions used for image classification. Typical visual explanation approaches include class activation mapping (CAM) (Zhou et al., 2016) and gradient weighted-CAM (Grad-CAM) (Ramprasaath et al., 2017). CAM outputs an attention map by utilizing the response of the convolution layer. Grad-CAM outputs an attention map by utilizing the positive gradients of a specific category. Attention branch network (ABN) (Fukui et al., 2019) that extends an attention map to an attention mechanism in order to improve the classification performance has also been proposed. Thanks to these visual explanation methods, the decision-making of CNNs is becoming clearer. However, we may not be able to get the desirable attention map corresponded to Ground Truth (GT). Examples of attention maps generated by Grad-CAM and ABN are shown in Fig. 1. Although the input image is annotated "Lakeland terrier" as a GT, it contains multiple objects: "Lakeland terrier" and "French bulldog". Therefore, if CNN pays attention to different objects than the GT, it is likely to perform incorrect classifications. This mismatch would be critical in some applications. For example, in medical image recognition systems, a mismatch between the classification result and the attention region would degrade the reliability of the classification.

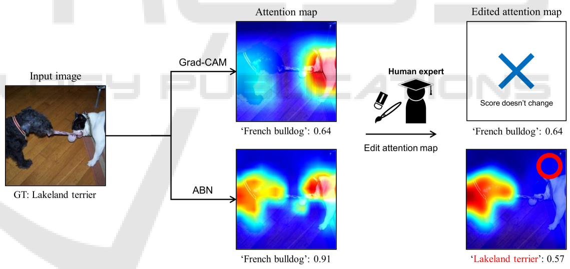

Figure 1: Adjustment of recognition result by editing an attention map on visual explanation.

To solve this issue, we aim to realize a method for embedding human knowledge into deep learning

Mitsuhara, M., Fukui, H., Sakashita, Y., Ogata, T., Hirakawa, T., Yamashita, T. and Fujiyoshi, H.
Embedding Human Knowledge into Deep Neural Network via Attention Map.
DOI: 10.5220/0010335806260636
In *Proceedings of the 16th International Joint Conference on Computer Vision, Imaging and Computer Graphics Theory and Applications (VISIGRAPP 2021) - Volume 5: VISAPP*, pages 626-636
ISBN: 978-989-758-488-6

models. Although this approach has been widely proposed (Branson et al., 2010; Deng et al., 2013; Branson et al., 2011; Parkash and Parikh, 2012; Parikh and Grauman, 2011; Duan et al., 2012), the conventional methods are based on rather small machine learning models comprising fewer model parameters, such as decision trees and conditional random fields (CRFs) (Quattoni et al., 2007). It is difficult to embed human knowledge into deep learning models due to the massive number of parameters.

In this paper, we propose a method for embedding human knowledge into deep learning models. The crucial factors leading the proposed method are an attention map for visual explanation and an attention mechanism, and we focus on ABN (Fukui et al., 2019). ABN applies an attention map for visual explanation to the attention mechanism. Therefore, by editing an attention map manually, as shown in Fig. 1, ABN can output a desirable recognition result by inference processing using the edited attention map. We propose a fine-tuning method based on the characteristics of ABN and an edited attention map. The proposed method fine-tunes the attention and perception branches of ABN to output the same attention map as the edited one. By learning the edited attention map that incorporates human knowledge, we can both obtain a more interpretable attention map and improve the recognition performance.

Our contributions are as follows:

- We demonstrate that manually editing the attention map used for a visual explanation can improve the recognition performance by reflecting human knowledge.
- We propose a fine-tuning method that uses manually edited attention maps. By training a network to output the same attention maps as the edited ones, we can embed human knowledge into deep neural networks.
- Beyond the visual explanation widely required in the development of deep neural networks, this paper formulates a novel optimization framework of networks that humans can intuitively edit via a visual interface. This will open new doors to future human-machine cooperation.

2 RELATED WORK

This section introduces studies on embedding human knowledge into machine learning methods and visual explanation on deep learning models.

2.1 Embedding Human Knowledge

One of the major approaches to embedding human knowledge into machine learning models is human-in-the-loop (HITL) (Branson et al., 2010; Deng et al., 2013; Branson et al., 2011; Parkash and Parikh, 2012; Parikh and Grauman, 2011; Duan et al., 2012). In HITL, human operators intervene during the training of machine learning. In the field of computer vision, HITL is often applied to difficult recognition tasks such as fine-grained recognition. Several feature extraction approaches based on human knowledge have been proposed (Branson et al., 2010; Duan et al., 2012; Deng et al., 2013).

Various kinds of human knowledge are introduced in HITL for fine-grained recognition. Branson *et al.* (Branson et al., 2010) proposed an interactive HITL approach that helps to train a decision tree by using a question and answer with respect to a specific bird. In addition to items inherent in an object, characteristic positions or regions of an object have also been used as human knowledge. Duan *et al.* (Duan et al., 2012) introduced the body part position and color of a bird as human knowledge into the training of a CRF. Deng *et al.* (Deng et al., 2013) used a bubble, that is, a circular bounding box, as human knowledge. This bubble information is annotated from an attention region when a user distinguishes the two types of birds. By annotating the bubble with various pairs and users, characteristic regions of bird images can be obtained when we recognize bird categories. These bubbles are introduced to the HITL framework as human knowledge, and can improve the accuracy of fine-grained recognition because the machine learning model is trained with an important location for recognizing the bird category. However, these methods have primarily been applied to models having a small number of parameters, and are rarely applied to deep learning. This is because deep learning has an enormous number of parameters.

Linsley *et al.* (Linsley et al., 2019) proposed a method that incorporates human knowledge into large-scale deep neural networks using the HITL framework. This method added a spatial attention mechanism into the attention mechanism (Luong et al., 2015; Kelvin et al., 2015; Hu et al., 2018; Bahdanau et al., 2016; Mnih et al., 2014; Wang et al., 2017; Vaswani et al., 2017; Wang et al., 2018; Yang et al., 2016; You et al., 2016; Woo et al., 2018) of squeeze-and-excitation networks (SENet) (Hu et al., 2018) and trained the network by using a ClickMe map that introduces human knowledge to the weights of the attention mechanism. This method can achieve higher accuracy because the network is trained while

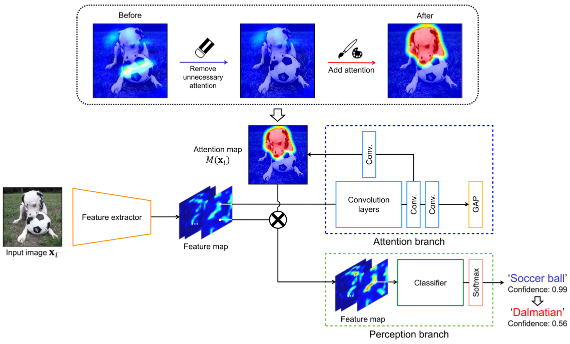

Figure 2: Editing procedure of an attention map.

Table 1: Top-1 and top-5 errors by edited attention map on validation samples on ImageNet dataset (1k) [%].

	top-1	top-5
Before editing	100.0	19.0
After editing	**83.2**	**15.8**

the attention mechanism weights located at multiple points become the same as the ClickMe map. Because the attention mechanism in (Linsley et al., 2019) is a channel-wise structure, attention maps are output for each feature map. It is difficult to edit an attention map when a human operator views the map subjectively. Meanwhile, we use a single-channel attention map for embedding human knowledge into deep neural networks. A human operator can understand the attention map intuitively and edit the map through a visual interface interactively. Therefore, our method demonstrates that humans can intuitively intervene into networks. In addition, Linsley *et al.*'s method learns end-to-end using pre-collected human attention regions, so there is no human intervention in the learning loop. In contrast, our network model is fine-tuned by editing the attention map that was misclassified by the pre-trained model, which trained only labels and images. Therefore, it is possible to directly and interactively embed human knowledge into the network model. This simple and intuitive solution is the strength of our method.

2.2 Visual Explanation

To interpret deep learning in computer vision, visual explanation that visualizes the discriminative region in the inference process has been used (Ribeiro et al., 2016; Chattopadhay et al., 2018; Ramprasaath et al., 2017; Smilkov et al., 2017; Zeiler and Fergus, 2014; Zhou et al., 2016; Fukui et al., 2019; Montavon et al., 2018; Springenberg et al., 2015; Fong and Vedaldi, 2017; Petsiuk et al., 2018; Jetley et al., 2018). Visual explanation can be categorized into two approaches: gradient-based, which outputs an attention map using gradients, and response-based, which outputs an attention map using the response of the convolutional layer. One of the gradient-based approaches is Grad-CAM (Ramprasaath et al., 2017), which can obtain an attention map for a specific category by using the response of the convolution layer and a positive gradient in the backpropagation process. Grad-CAM can be applied to various pre-trained models.

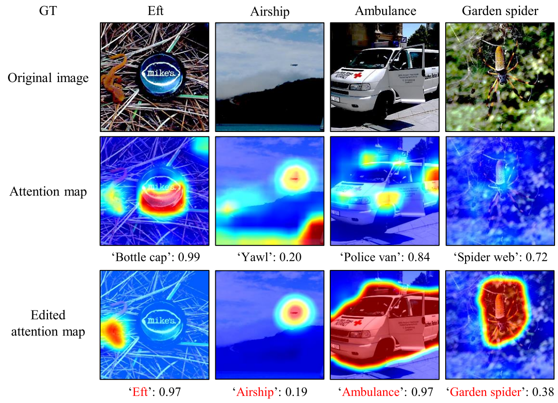

Figure 3: Example of conventional and edited attention maps.

One of the response-based approaches is CAM (Zhou et al., 2016), which outputs an attention map by using a K channel feature map from the convolution layer of each category. The attention maps of each category are calculated by using the K channel feature map and the weight at a fully connected layer. However, CAM degrades the recognition accuracy because spatial information is removed due to the global average pooling (GAP) (Lin et al., 2014) layer between the convolutional and fully connected layers. To address this issue, ABN has been proposed (Fukui et al., 2019), which extends an attention map for the visual explanation to an attention mechanism. By applying an attention map to the attention mechanism, ABN improves the classification performance and obtains an attention map simultaneously.

In this paper, we focus on this ABN ability. Because of the attention mechanism, ABN can adjust recognition results by considering the manually edited attention map. Moreover, we propose a method for embedding human knowledge into the network by fine-tuning so that the edited attention map and the attention map obtained from ABN become the same.

3 INVESTIGATION OF EDITING ATTENTION MAP

We believe editing an attention map has a potential to adjust the recognition result. In this section, we investigate the behavior of ABN in a case where we edit an attention map manually. Specifically, we confirm the changes in classification performance by editing an attention map on the ImageNet dataset (Deng et al., 2009).

3.1 Editing of Attention Map

We used an ABN whose backbone is 152-layer ResNet (He et al., 2016) (ResNet-152+ABN) as a network model. ResNet-152+ABN is trained with $1,200$k training samples from the ImageNet dataset. Then, we selected the 1k misclassified samples from the validation samples and edited their attention maps.

Figure 2 shows the editing procedure of an attention map. We first input a misclassified sample to ResNet-152+ABN and obtain the attention map from the attention branch, where the size of the attention map is 14×14 pixels. Then, we edit the obtained attention map manually. Note that the attention map is resized to 224×224 pixels and is overlaid with the input image for ease of manual editing. The edited attention map is resized to 14×14 pixels and used for an attention mechanism to infer classification results from the perception branch. In the example shown in Fig. 2, the attention map obtained from ResNet-152+ABN classifies the input image as “Soccer ball” and also highlights the corresponding object. By editing the attention map to highlight “Dalmatian” and using it for the attention mechanism, the classification result is successfully adjusted to “Dalmatian”.

Examples of the edited attention map are provided in Fig. 3. In the two left columns, images contain objects from multiple categories and ResNet-152+ABN misclassifies these images due to focusing on different objects. For example, in the first column, although the GT is “Eft”, ResNet-152+ABN recognizes “Bottle cap”, because the attention map highlights the “Bottle cap”. By removing the attention region of “Bottle cap” and adding the attention to “Eft”, the recognition result of ABN is changed to “Eft”. In the second column, ResNet-152+ABN also misclassifies to “Yawl” because the attention map highlights both “Airship” and “Yawl”. By removing the attention location of “Yawl”, we can adjust the recognition result to “Airship”. Meanwhile, in the two right columns, the attention maps do not highlight the entire objects and incorrect classification results are provided. By editing the attention maps to highlight the entire objects, the classification results are adjusted correctly.

We show the top-1 and top-5 errors before and after editing the attention map in Tab. 1. Here, the top-1 error before editing is 100% because the 1,000 validation samples we used are collected from false recognition on the top-1 recognition result. We can reduce the top-1 error by 16.8% by editing the attention maps. In the top-5 error, we can also reduce from 19.0% to 15.8%.

4 PROPOSED METHOD

We discuss how to embedding human knowledge into deep neural networks. The results discussed in Sec. 3 demonstrate that the recognition result of ABN can be adjusted by editing the attention map. This suggests that ABN can be applied to embedding human knowledge into the network. Therefore, we propose fine-tuning the attention and perception branches of ABN by using the edited attention map. By training the attention and perception branches with the edited attention map including human knowledge, ABN can output an attention map that considers this knowledge and thereby improve the classification performance.

4.1 Embedding Human Knowledge via Edited Attention Map

The flow of the proposed method is shown in Fig. 4. First, an ABN model is trained using training samples with labels, and then we collect the attention maps of these samples from the trained model. We only collect the attention maps of misclassified training samples. Second, we edit each of the attention map based on human knowledge to recognize them correctly. Third, the attention and perception branches of ABN are fine-tuned with the edited attention maps. During the fine-tuning process, we update the parameters of the attention and perception branches by using the loss of ABN and a loss calculated from the attention map output from ABN and the edited one (the details are described in Sec. 4.3).

4.2 Manual Edit of Attention Map

We introduce the three methods to edit attention maps depending on the dataset.

ImageNet Dataset. We manually edit the attention maps of the ImageNet dataset with the same process as described in Sec. 3. To edit as many attention maps as possible, we created a tool that can edit attention maps interactively, as shown in Fig. 6. This tool can add (Fig. 6(a)) and remove (Fig. 6(b)) an attention region simply by dragging the mouse. With this tool, we can edit attention maps interactively while verifying the top-3 classification results. Examples of the edited attention maps are shown in Fig. 5(a). These

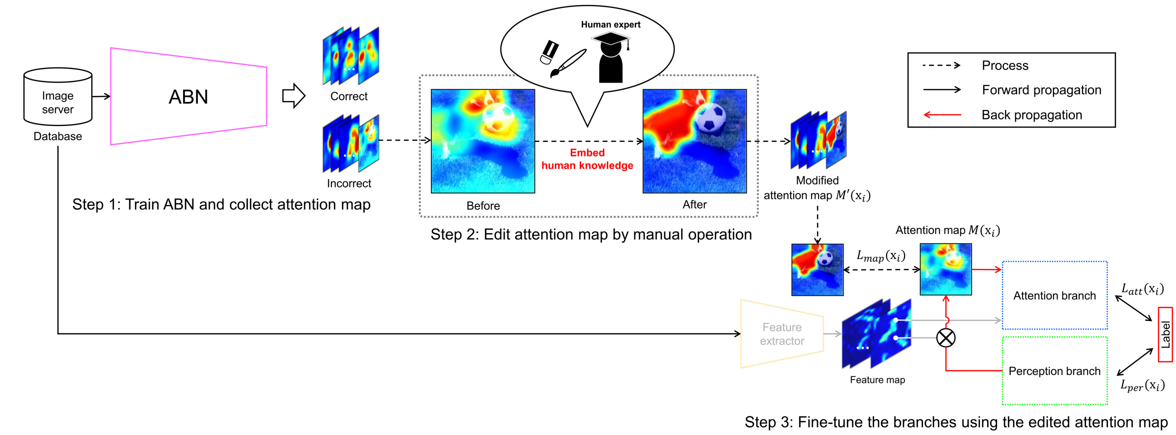

Figure 4: Process flow of the proposed method.

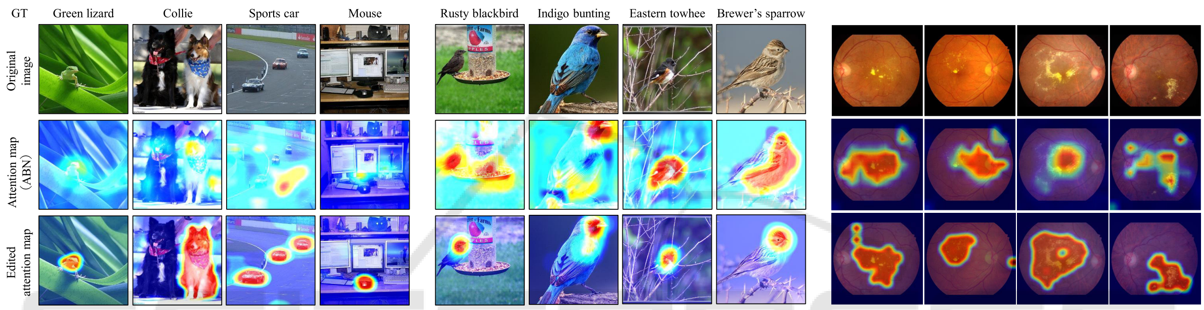

(a) ImageNet (b) CUB-200-2010 (c) IDRiD

Figure 5: Example of edited attention map for each dataset.

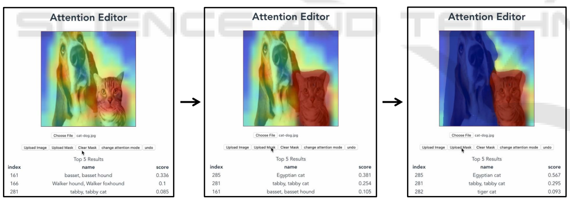

Before editing attention (a) Add (b) Remove

Figure 6: Attention map editor tool. (a) Addition of attention. (b) Removal of attention.

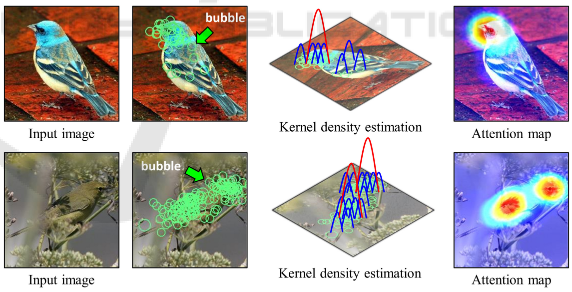

Figure 7: Making an attention map from the bubble by kernel density estimation.

maps are edited so that an object or characteristic region with respect to the GT is highlighted [1].

CUB-200-2010 Dataset. In the CUB-200-2010 dataset (Welinder et al., 2010), we embed human knowledge into an attention map by using bubble information (Deng et al., 2013). The bubble information represents the attention region by means of the position and scale of the circular bounding box when multiple users distinguish two categories of birds. This information is an important human knowledge to recognize the multiple categories of birds. For this reason, we make an attention map with human knowledge from the bubble information.

For each bird image, bubbles are annotated by multiple users. The number of bubbles given by one user is not limited. To make an attention map from the bubbles, we use a kernel density estimation with multiple bubbles, as shown in Fig. 7. A dense region of bubbles indicates an important region for recognizing the bird category. The density of bubble information enables us to obtain the attention map embedded with human knowledge, as shown in Fig. 5(b). The map is then normalized to [0-1] and used for the proposed fine-tuning method.

[1]This tool is available at https://github.com/machine-perception-robotics-group/AttentionEditorABN.

Fundus Image Dataset (IDRiD). To achieve an automatic diagnosis, medical image recognition has been attempted for various recognition tasks, such as retinal disease recognition (Jeffrey et al., 2018) and risk forecasting of heart disease (Ryan et al., 2018). In actual medical practice, a system that can explain the reason behind a decision is required in order to enhance the reliability of the diagnosis. The presentation of decision-making in automatic diagnosis is attracting considerable attention because automatic diagnosis is greatly helpful to doctors when making a diagnosis. In this paper, we evaluate the disease recognition of a fundus image.

For this disease recognition, we use the Indian Diabetic Retinopathy Image Dataset (IDRiD) (Porwal et al., 2018). IDRiD is concerned with the disease grade recognition of retina images, and the presence or absence of diseases is recognized from exudates and hemorrhages. IDRiD includes a segmentation label of disease regions annotated by a specialist, as shown in Fig. 5(c). We edit the attention map of the disease classification task by using the segmentation label.

4.3 Fine-tuning of the Branches

After editing attention maps including human knowledge, ABN is fine-tuned with these maps. In the proposed fine-tuning method, we formulate the loss function L in addition to the conventional ABN loss function L_{abn}. Let $\mathbf{x}_i$ be the i-th sample in the training dataset. The loss function of ABN is calculated by

$$L_{abn}(\mathbf{x}_i) = L_{att}(\mathbf{x}_i) + L_{per}(\mathbf{x}_i), \qquad (1)$$

where L_{att} and L_{per} are conventional cross entropy losses for the attention and perception branches, respectively. The loss function of the fine-tuning $L(\mathbf{x}_i)$ is defined as

$$L(\mathbf{x}_i) = L_{abn}(\mathbf{x}_i) + L_{map}(\mathbf{x}_i). \qquad (2)$$

As the loss of the attention maps L_{map}, we use the L2 norm between the two attention maps. We denote an output attention map from ABN and a edited attention map as $M(\mathbf{x}_i)$ and $M'(\mathbf{x}_i)$, respectively. The attention map loss L_{map} are formulated by

$$L_{map}(\mathbf{x}_i) = \gamma \|M'(\mathbf{x}_i) - M(\mathbf{x}_i)\|_2, \qquad (3)$$

where γ is a scale factor. Typically, L_{map} is larger than L_{att} and L_{per}. Hence, we adjust the effect of $L_{map}(\mathbf{x}_i)$ by scaling L_{map} with γ.

By introducing L_{map}, ABN is optimized so that an output attention map is close to the edited attention map including human knowledge. In this way, we can embed human knowledge into a network via the edited attention map. During the fine-tuning, the proposed method optimizes the attention and perception branches of ABN. The feature extractor that extracts the feature map from an input image is not updated during the fine-tuning process.

5 EXPERIMENTS

We evaluate the proposed method on image classification (Deng et al., 2009), fine-grained recognition (Welinder et al., 2010), and fundus image classification (Porwal et al., 2018) tasks. Also, in order to quantitatively evaluate the explanation capability of the attention map, we use the deletion metric, the insertion metric, and the degree of similarity between the edited attention map and the attention map output by the network.

5.1 Experimental Details

ImageNet Dataset. We collect misclassified training samples of the top-1 result in the ImageNet dataset to edit the attention map and to use for fine-tuning. We edit the attention maps of 100 categories with lower classification performance to evaluate the improvement and randomly selected ten categories among them. The number of edited attention maps was 30,917, and editing was performed by 43 users. During fine-tuning, we compare two training performances: training only ten categories and training all 100 categories of the edited attention maps.

Our baseline models are ResNet-18, ResNet-34, ResNet-50, and ResNet-152 that includes a SENet (Hu et al., 2018). We used the same learning conditions as (Fukui et al., 2019).

CUB-200-2010 Dataset. The CUB-200-2010 dataset includes attention maps created by the bubble information for all training samples. Therefore, the training samples are sorted by their confidence, and the samples are used for fine-tuning from the lowest confidence.

Since the CUB-200-2010 dataset has a small number of samples, it is easy for over-fitting to occur, and learning from scratch is difficult. For this reason, we evaluated two learning methods: training from scratch and fine-tuning the pre-trained model on ImageNet. These models are trained by SGD with momentum in 300 epochs. The learning rate is decreased to 0.1 times at 150 and 225 epochs. The mini-batch size is 16.

IDRiD. IDRiD contains 81 diseased images and 120 healthy images based on the existence of hemorrhages, hard exudates, and soft exudates. We create

Table 2: Top-1 error rates on ImageNet dataset [%].

No. of categories	Model	top-1 error
10 random categories	ResNet-18	9.00
	ResNet-34	9.60
	ResNet-50	12.00
	ResNet-18+ABN	8.40
	ResNet-34+ABN	7.60
	ResNet-50+ABN	11.20
	Proposed (ResNet-18+ABN)	**6.20**
	Proposed (ResNet-34+ABN)	**7.40**
	Proposed (ResNet-50+ABN)	**10.80**
100 worst categories	ResNet-152	31.90
	ResNet-152+SE+ABN	31.16
	Proposed (ResNet-152+SE+ABN)	**30.88**

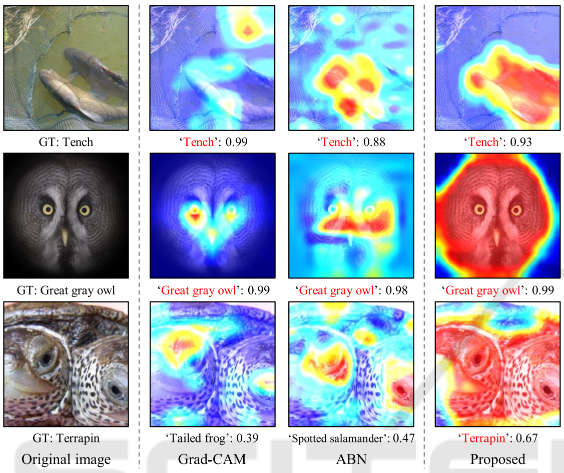

Figure 8: Examples of conventional and proposed attention maps on ImageNet dataset.

the edited attention maps by using semantic segmentation labels annotated by medical doctors. We evaluate IDRiD by 5-fold cross validation. Our baseline models are an AlexNet, ResNet-18, ResNet-34 and ResNet-50-based CNNs. The networks are trained by SGD with momentum, and the number of training iterations is 9,500 epochs. The batch size is 20 and the size of each image is 360 $\times$ 360 pixels. Data augmentation is as follows: mirroring, intensity change, scaling, and rotation.

Quantitative Evaluation of Attention Map. In order to quantitatively evaluate the explainability of the attention map, we employ the deletion metric, the insertion metric, and the degree of similarity between the edited attention map and the attention map output by the network. The deletion and insertion metrics are evaluation methods proposed by Petsiuk *et al.* (Petsiuk et al., 2018), which are based on the concept of literature (Fong and Vedaldi, 2017). The deletion metric measures the decrease of score by gradually deleting the high attention area of an attention map from the input image. Therefore, a lower score means a higher explanation. On the other hand, the insertion metric measures the increase of score by gradually inserting the high attention area of an attention map in the input image. Therefore, a higher score means a higher explanation. In the evaluation, the degree of similarity between the edited attention map and the attention map output by the network is measured by the mean square error. A higher similarity (i.e., lower error) means that the attention map focuses on the same area as the human operator and thus successfully embedded human knowledge.

Table 3: Top-1 and top-5 accuracies on CUB-200-2010 dataset [%].

Model	scratch top-1	scratch top-5	pre-trained top-1	pre-trained top-5
Deng's method	32.80	–	–	–
ResNet-18	28.38	52.62	62.58	83.25
ResNet-34	27.39	53.28	67.59	85.13
ResNet-50	28.02	54.33	69.27	88.39
ResNet-18+ABN	32.38	57.27	63.57	83.45
ResNet-34+ABN	30.99	53.68	68.25	87.73
ResNet-50+ABN	31.68	57.01	71.68	89.09
Proposed (ResNet-18+ABN)	**36.96**	**61.66**	**64.72**	**83.71**
Proposed (ResNet-34+ABN)	**38.15**	**62.78**	**69.27**	**87.88**
Proposed (ResNet-50+ABN)	**37.42**	**62.08**	**72.07**	**90.37**

5.2 Image Classification on ImageNet

We evaluated the classification performance by using the 100 worst categories and randomly select ten categories on the ImageNet dataset as in the previous evaluation. The accuracies of the conventional ResNet and the proposed method for ten and 100 categories are listed in Tab. 2. As shown, the accuracy of the proposed method is higher than that of the conventional ABN.

The attention maps of the conventional and proposed methods are shown in Fig. 8. The attention map of the conventional ABN is noisy or focuses on different objects, which results in wrong classifications. In contrast, the proposed method can obtain a clear attention map that highlights the target category object, thus improving the classification performance.

5.3 Fine-grained Recognition on CUB-200-2010

We compared the accuracies of Deng *et al.*, the conventional ResNet, and the proposed method for top-1 and top-5 accuracy. The results are shown in Tab. 3. The performances of the conventional ABN trained from scratch and the Deng's method are the same. By fine-tuning the ABN using an attention map with human knowledge, the top-1 accuracies are improved from 4% to 7% in the case of scratch. Also, in the case of the pre-trained model on ImageNet, the accuracies are improved by about 1%. Similarly, in the recognition accuracy of top-5, the recognition rate improved

Table 4: Comparison of the deletion (lower is better) and insertion (higher is better) scores of conventional visual explanation and proposed method on CUB-200-2010 dataset.

	ResNet-18		ResNet-34		ResNet-50	
Method	Deletion	Insertion	Deletion	Insertion	Deletion	Insertion
Grad-CAM	**0.2247**	0.2546	0.3147	0.2540	0.3688	0.2378
ABN	0.3146	0.2269	0.2920	0.3596	0.2915	0.4033
Proposed	0.2568	**0.3268**	**0.2609**	**0.3956**	**0.2722**	**0.4575**

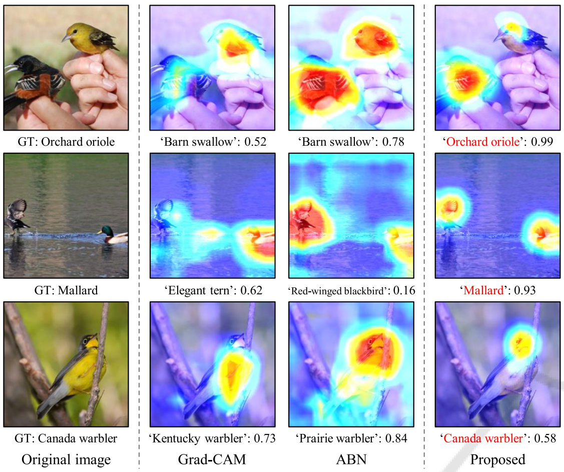

Figure 9: Examples of conventional and proposed attention maps on CUB-200-2010 dataset.

Table 5: Comparison of the similarity of the attention map by mean square error of the conventional visual explanation and proposed method on CUB-200-2010 dataset.

Method	ResNet-18	ResNet-34	ResNet-50
CAM	0.6456	0.7658	0.6031
Grad-CAM	0.4502	0.4831	0.3875
ABN	0.1682	0.3022	0.5499
Proposed	**0.1136**	**0.1597**	**0.2049**

from about 4% to 9% in the case of scratch, and about 1% for the pre-trained model on ImageNet.

Examples of the obtained attention map on the fine-grained recognition are shown in Fig. 9. The conventional ABN highlights the entire body of the bird. In contrast, the proposed method highlights the local characteristic regions, such as the color and the head of the bird. In addition, the proposed method removes noise from the attention map by fine-tuning. Thus, the proposed method can also improve the performance of fine-grained recognition.

For the quantitative evaluation on the explainability of the attention map, we show the deletion (lower is better) and insertion (higher is better) scores of the conventional and proposed methods for test samples of CUB-200-2010 dataset in Tab. 4. As shown, the proposed method has higher scores than the other methods. In other words, the proposed method provides the clearest visual explanation of all the methods.

Table 6: Comparison of the accuracy on IDRiD [%].

Model	Accuracy
AlexNet	89.66
ResNet-18	89.78
ResNet-34	94.44
ResNet-50	95.83
AlexNet+ABN	93.11
ResNet-18+ABN	95.33
ResNet-34+ABN	96.88
ResNet-50+ABN	97.22
Proposed (AlexNet+ABN)	**96.78**
Proposed (ResNet-18+ABN)	**96.88**
Proposed (ResNet-34+ABN)	**97.23**
Proposed (ResNet-50+ABN)	**99.17**

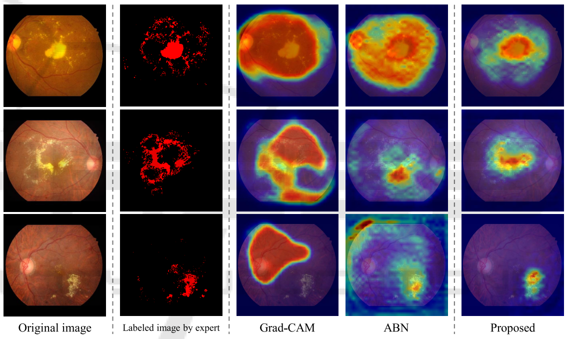

Figure 10: Examples of conventional and proposed attention maps on IDRiD.

In Table 5, we compare the degree of similarity between the attention maps output by the conventional visual explanation method and the proposed method and the attention maps created by bubble information. As shown in the table, the proposed method outputs the attention map that is closest to the one created by the bubble information. These results demonstrate that the proposed method can successfully embed human knowledge and output an attention map that contains this knowledge.

5.4 Fundus Image Classification on IDRiD

Table 6 shows the classification accuracies on IDRiD. As shown, the ABN-based networks (e.g., AlexNet+ABN, ResNet∗+ABN) achieved higher classification performances than the original networks. Moreover, the classification performances are

Table 7: Comparison of the deletion (lower is better) and insertion (higher is better) scores of the conventional visual explanation and the proposed method on IDRiD.

Method	ResNet-18		ResNet-34		ResNet-50	
	Deletion	Insertion	Deletion	Insertion	Deletion	Insertion
Grad-CAM	0.6296	0.3307	0.5979	0.4286	**0.4841**	0.3307
ABN	0.5741	0.8016	0.5556	0.8307	0.5503	0.8175
Proposed	**0.5132**	**0.9153**	**0.5132**	**0.9233**	0.5000	**0.9259**

Table 8: Comparison of the similarity of the attention map by mean square error of the conventional visual explanation and proposed method on IDRiD.

Method	ResNet-18	ResNet-34	ResNet-50
CAM	0.3749	0.3300	0.2287
Grad-CAM	0.1521	0.1329	0.1532
ABN	0.1241	0.1309	0.1286
Proposed	**0.0893**	**0.0927**	**0.0904**

further improved by introducing the proposed fine-tuning method.

Figure 10 shows examples of the resultant attention maps. In the case of the conventional Grad-CAM, the attention maps broadly highlight both disease and non-disease regions. Also, the conventional ABN focuses on the non-disease regions around the disease regions. In contrast, the proposed method suppresses the highlighting for non-disease regions and focuses only on disease regions.

We evaluate the obtained attention maps quantitatively. Tables 7 and 8 show that deletion and insertion scores and the similarity of the attention maps, respectively. As shown in the Table 7, the proposed method has higher insertion scores than the other methods. As shown in the Table 8, the proposed method outputs the attention map that is closest to the one edited by a segmentation label of disease regions annotated by a specialist. These results demonstrate that the proposed method is effective for fundus image recognition, where it is difficult to collect a large amount of training data, and that the interpretability of the attention map can be improved.

6 CONCLUSION

We proposed an approach to embed human knowledge into deep learning models by fine-tuning the network with a manually edited attention map. Specifically, the proposed method fine-tunes the ABN by calculating the training loss between the output attention map and the edited attention map. By fine-tuning using a manually edited attention map by a human expert, we can embed human knowledge into the network and obtain an appropriate attention map for better visual explanation. Moreover, by introducing human knowledge to the attention map, classification performance is improved. Experimental results with ImageNet, CUB-200-2010, and IDRiD showed that the proposed method improved the classification accuracies. Our evaluation of the attention maps showed that the proposed method obtained better deletion and insertion scores than conventional methods. Moreover, the similarity score results show that the proposed method can provides attention maps that are similar to the edited by a human expert. Consequently, our method can generate a more interpretable attention map and successfully embed human knowledge. Our future work will include further improvement of the performance by editing attention maps with multi-resolution.

ACKNOWLEDGEMENTS

This paper is based on results obtained from a project, JPNP20006, commissioned by the New Energy and Industrial Technology Development Organization (NEDO).

REFERENCES

Bahdanau, D., Cho, K., and Bengio, Y. (2016). Neural machine translation by jointly learning to align and translate. In *International Conference on Learning Representations*.

Branson, S., Perona, P., and Belongie, S. (2011). Strong supervision from weak annotation: Interactive training of deformable part models. In *2011 International Conference on Computer Vision*, pages 1832–1839.

Branson, S., Wah, C., Schroff, F., Babenko, B., Welinder, P., Perona, P., and Belongie, S. (2010). Visual recognition with humans in the loop. In *European Conference on Computer Vision*, pages 438–451.

Chattopadhay, A., Sarkar, A., Howlader, P., and Balasubramanian, V. N. (2018). Grad-CAM++: Generalized gradient-based visual explanations for deep convolutional networks. In *2018 IEEE Winter Conference on Applications of Computer Vision*, pages 839–847.

Deng, J., Dong, W., Socher, R., Li, L.-J., Li, K., and Fei-Fei, L. (2009). Imagenet: A large-scale hierarchical image database. In *2009 IEEE Conference on Computer Vision and Pattern Recognition*, pages 248–255.

Deng, J., Krause, J., and Fei-Fei, L. (2013). Fine-grained crowdsourcing for fine-grained recognition. In *2013*

IEEE Conference on Computer Vision and Pattern Recognition, pages 580–587.

Duan, K., Parikh, D., Crandall, D., and Grauman, K. (2012). Discovering localized attributes for fine-grained recognition. In *2012 IEEE Conference on Computer Vision and Pattern Recognition*, pages 3474–3481.

Fong, R. C. and Vedaldi, A. (2017). Interpretable explanations of black boxes by meaningful perturbation. In *2017 IEEE International Conference on Computer Vision*, pages 3429–3437.

Fukui, H., Hirakawa, T., Yamashita, T., and Fujiyoshi, H. (2019). Attention branch network: Learning of attention mechanism for visual explanation. In *2019 IEEE Conference on Computer Vision and Pattern Recognition*, pages 10705–10714.

He, K., Zhang, X., Ren, S., and Sun, J. (2016). Deep residual learning for image recognition. In *2016 IEEE Conference on Computer Vision and Pattern Recognition*, pages 770–778.

Hu, J., Shen, L., and Sun, G. (2018). Squeeze-and-excitation networks. In *2018 IEEE Conference on Computer Vision and Pattern Recognition*, pages 7132–7141.

Jeffrey, De, F., Joseph, R., L., Bernardino, R.-P., Stanislav, N., Nenad, T., Sam, B., Harry, A., Xavier, G., Brendan, O., Daniel, V., George, van, d. D., Balaji, L., Clemens, M., Faith, M., Simon, B., Kareem, A., Reena, C., Dominic, K., Alan, K., Cían, O., H., Rosalind, R., Julian, H., Dawn, A., S., Catherine, E., Adnan, T., Hugh, M., Demis, H., Geraint, R., Trevor, B., Peng, T., K., Mustafa, S., Julien, C., Pearse, A., K., and Olaf, R. (2018). Clinically applicable deep learning for diagnosis and referral in retinal disease. *Nature Medicine*, (24):1342–1350.

Jetley, S., Lord, N. A., Lee, N., and Torr, P. (2018). Learn to pay attention. In *International Conference on Learning Representations*.

Kelvin, X., Jimmy, B., Ryan, K., Kyunghyun, C., Aaron, C., Ruslan, S., Rich, Z., and Yoshua, B. (2015). Show, attend and tell: Neural image caption generation with visual attention. In *International Conference on Machine Learning*, pages 2048–2057.

LeCun, Y., Boser, B., Denker, J. S., Henderson, D., Howard, R. E., Hubbard, W., and Jackel, L. D. (1989). Backpropagation applied to handwritten zip code recognition. *Neural Computation*, 1(4):541–551.

Lin, M., Chen, Q., and Yan, S. (2014). Network in network. In *2nd International Conference on Learning Representations, Banff, AB, Canada, April 14-16, 2014, Conference Track Proceedings*.

Linsley, D., Shiebler, D., Eberhardt, S., and Serre, T. (2019). Learning what and where to attend with humans in the loop. In *International Conference on Learning Representations*.

Luong, T., Pham, H., and Manning, C. D. (2015). Effective approaches to attention-based neural machine translation. In *Empirical Methods in Natural Language Processing*, pages 1412–1421.

Mnih, V., Heess, N., Graves, A., and kavukcuoglu, k. (2014). Recurrent models of visual attention. In *Neural Information Processing Systems*, pages 2204–2212.

Montavon, G., Samek, W., and Müller, K.-R. (2018). Methods for interpreting and understanding deep neural networks. *Digital Signal Processing*, 73:1–15.

Parikh, D. and Grauman, K. (2011). Interactively building a discriminative vocabulary of nameable attributes. In *2011 IEEE Conference on Computer Vision and Pattern Recognition*, pages 1681–1688.

Parkash, A. and Parikh, D. (2012). Attributes for classifier feedback. In *European Conference on Computer Vision*, pages 354–368.

Petsiuk, V., Das, A., and Saenko, K. (2018). Rise: Randomized input sampling for explanation of black-box models. In *British Machine Vision Conference*.

Porwal, P., Pachade, S., Kamble, R., Kokare, M., Deshmukh, G., Sahasrabuddhe, V., and Meriaudeau, F. (2018). Indian diabetic retinopathy image dataset (idrid): A database for diabetic retinopathy screening research. *Data*, 3:25.

Quattoni, A., Wang, S., Morency, L.-P., Collins, M., and Darrell, T. (2007). Hidden conditional random fields. *IEEE Transactions on Pattern Analysis & Machine Intelligence*, (10):1848–1852.

Ramprasaath, R., S., Michael, C., Abhishek, D., Ramakrishna, V., Devi, P., and Dhruv, B. (2017). Grad-CAM: Visual explanations from deep networks via gradient-based localization. In *International Conference on Computer Vision*, pages 618–626.

Ribeiro, M. T., Singh, S., and Guestrin, C. (2016). Why should I trust you?: Explaining the predictions of any classifier. In *22nd ACM SIGKDD International Conference on Knowledge Discovery and Data Mining*, pages 1135–1144.

Ryan, P., Avinash, V., V., Katy, B., Yun, L., Michael, V., M., Greg, S., C., Lily, P., and Dale, R., W. (2018). Prediction of cardiovascular risk factors from retinal fundus photographs via deep learning. *Nature Biomedical Engineering*, (2):158–164.

Smilkov, D., Thorat, N., Kim, B., Viégas, F., and Wattenberg, M. (2017). Smoothgrad: removing noise by adding noise. *arXiv preprint arXiv:1706.03825*.

Springenberg, J. T., Dosovitskiy, A., Brox, T., and Riedmiller, M. A. (2015). Striving for simplicity: The all convolutional net. In *International Conference on Learning Representations*.

Vaswani, A., Shazeer, N., Parmar, N., Uszkoreit, J., Jones, L., Gomez, A. N., Kaiser, Ł., and Polosukhin, I. (2017). Attention is all you need. In *Advances in Neural Information Processing Systems*, pages 5998–6008.

Wang, F., Jiang, M., Qian, C., Yang, S., Li, C., Zhang, H., Wang, X., and Tang, X. (2017). Residual attention network for image classification. In *2017 IEEE Conference on Computer Vision and Pattern Recognition*, pages 3156–3164.

Wang, X., Girshick, R., Gupta, A., and He, K. (2018). Non-local neural networks. In *2018 IEEE Conference* *on Computer Vision and Pattern Recognition*, pages 7794–7803.

Welinder, P., Branson, S., Mita, T., Wah, C., Schroff, F., Belongie, S., and Perona, P. (2010). Caltech-UCSD Birds 200. Technical Report CNS-TR-2010-001, California Institute of Technology.

Woo, S., Park, J., Lee, J.-Y., and So Kweon, I. (2018). Cbam: Convolutional block attention module. In *European Conference on Computer Vision*, pages 3–19.

Yang, Z., He, X., Gao, J., Deng, L., and Smola, A. (2016). Stacked attention networks for image question answering. In *2016 IEEE Conference on Computer Vision and Pattern Recognition*, pages 21–29.

You, Q., Jin, H., Wang, Z., Fang, C., and Luo, J. (2016). Image captioning with semantic attention. In *2016 IEEE Conference on Computer Vision and Pattern Recognition*, pages 4651–4659.

Zeiler, M. D. and Fergus, R. (2014). Visualizing and understanding convolutional networks. In *European Conference on Computer Vision*, pages 818–833.

Zhou, B., Khosla, A., Lapedriza, A., Oliva, A., and Torralba, A. (2016). Learning deep features for discriminative localization. In *2016 IEEE Conference on Computer Vision and Pattern Recognition*, pages 2921–2929.